



POWER VARIATION ANALYSIS OF ECHO SIGNAL FROM IONOSPHERIC REFLECTOR

Cesidio Bianchi, Marco Pietrella, Enrico Zuccheretti, Baskaradas James Arokiasamy, Vincenzo Romano, Umberto Sciacca
 Istituto Nazionale di Geofisica e Vulcanologia, Rome, Italy e-mail:bianchi@ingv.it



GP2 - 06.2

Abstract

A series of measurements of the radio echo power was performed to study and to monitor some dynamic characteristics of the ionospheric reflector. The sounding system was derived from a phase coded HF radar with the purpose of studying the ionospheric fading channel under certain controlled conditions. The single fixed frequency sounding that lasts a few minutes is carried out between two ionospheric vertical soundings to validate the chosen reflector. This work presents the experimental set-up and some preliminary results of the measurements.

Experimental setup

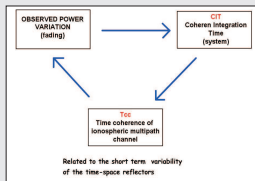


Figure 1

The idea is to study the behavior of the ionospheric channel exploiting the parametric integration capability of the AIS-INGV ionosonde. When the integration time is greater than the ionospheric coherence time the integration process is not so efficient giving a measured power smaller than the expected one.

The modern ionosondes (low power HF coded waveform bi-static radar) generally operate with transmitting power of about hundreds of watts and employ low gain long wire rhombic or delta antennas. The experimental set-up utilizes the ionosonde AIS-INGV as in normal vertical sounding configuration operating at fixed frequency, once the presence of ionospheric layer has been ascertained by previous measurements.

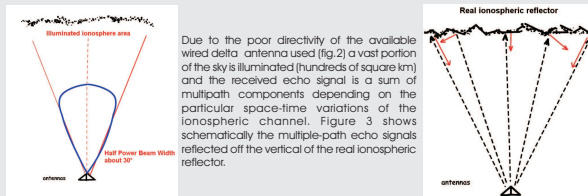


Figure 2

Figure 3

Due to the poor directivity of the available wired delta antenna used (fig.2) a vast portion of the sky is illuminated (hundreds of square km) and the received echo signal is a sum of multipath components depending on the particular space-time variations of the ionospheric channel. Figure 3 shows schematically the multiple-path echo signals reflected off the vertical of the real ionospheric reflector.

$$A(t) = u_e(t) \cos(2\pi f_c t)$$

Emitted signal where:
 $A(t)$ is the time dependent amplitude,
 $u_e(t)$ the waveform of the HF radar signal that contains the phase code,
 f_c is the carrier frequency.

Received signal.
 The sum of the s reflectors takes into account the possible paths and can vary during the measurement from D to $N(f)$
 α_s is the attenuated s-path containing the code,
 τ_s is the delay,
 φ_{ds} is the time dependent Doppler phase shift,
 $n(t)$ is the noise.

Baseband signal.
 By neglecting φ_{ds} and $n(t)$ what remains is an attenuated multipath path with time of arrival of the different components, whose phases can interfere in destructive/non-destructive ways that are responsible of the short term power variation. The moving reflectors introduce a short time variability fading because of the Doppler harmonics; this affects also the CIT and the Doppler bandwidth. The in-phase and quadrature sampling of the signal produces time discrete sequences on which the analysis was performed.

$$r(t) = \sum_{s=1}^{N(f)} \alpha_s(t - \tau_s(t)) \cos(\varphi_{ds}(t)) + n(t)$$

Analysis method

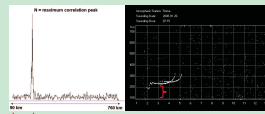


Figure 4

The output of the system is a time domain series exhibiting a peak in the position of the main reflector which amplitude is related to the reflected power.

Operating at fixed frequency we start a measurement session lasting around 350 s every 15 minutes. During this time the peaks are integrated along 0.5 s integration time (CI), storing the intensity in dBm and virtual height in km. The result is a time series of backscattered power as in fig. 5. We repeated these measurements along several days recording an ionogram before and after every session.



Figure 5

The idea is to divide the original time series into sub intervals where to look for the stability conditions; intervals in which power fluctuations are within a pre-fixed threshold. An analysis algorithm has been created exploiting the standard deviation as an indicator of the distribution of power values around the average one in the chosen interval.
 Every point in the original series becomes a starting point for a T second interval where we calculate a getting a derivate series. So $\alpha_s(t)$ indicates the t is the starting point for a T seconds interval where 95% of the power values are within $\pm 2\sigma$.

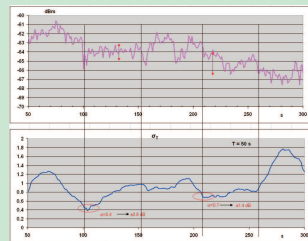


Figure 6

A more sophisticated analysis aims to find the longest continuous stability intervals so to understand how stability intervals are distributed along the measurement session.

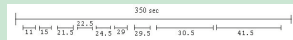


Figure 7

First result

The first application was to analyze the distribution of the ionospheric stability along the day using values from 20 days measurements, from 3 January to 22 January 2008.
 The aim of the analysis is to highlight stability intervals inside the session according to some defined thresholds. Particularly in our first trials we consider the ionosphere stable when power variations are smaller than ± 1 dB and virtual height variations are within the vertical resolution (around 5 km).
 We operated at a frequency of 3.00 MHz being the session 350s long.

For every session in each day we counted the stability intervals adding together the results for the sessions belonging to the same hour. Then the contributions of every day have been properly summed to obtain the distribution along 24 hours. We studied the ionospheric fading along 5 s and 10 s interval (figures. 8 and 9).

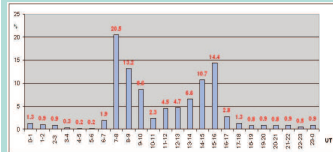


Figure 8. Distribution of occurrence percentage of 5 s stabilities.



Figure 9. Distribution of occurrence percentage of 10 s stabilities.

Both the distributions are very similar exhibiting relative minima and maxima. We can try to explain the different behavior of the two distributions.
 Around 4-5 UT the 5 s distribution presents a minimum due to the rise time considered at ionospheric altitude. The 10 s distribution also shows a minimum around the same hours due to the rise time.
 The abrupt variation around 10-11 UT can be caused by the sun set.
 The minimum around 10-11 UT and the low percentage values during the night can be explained looking at the same sample of ionograms in those hours

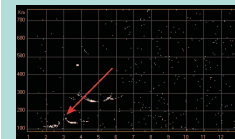


Figure 10

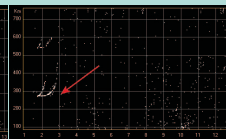


Figure 11

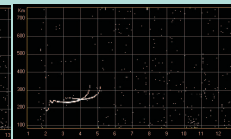


Figure 12

The minimum presented by both cases of 5s and 10s around 10-11 am UT is due to the fact that the chosen frequency corresponds to a cusp or critical frequency.
 During the night we recorded very low numbers of stability events because very often the sounding frequency was higher than the critical frequency.
 The maximum value around 7-8 am and 15-16 UT are due to the fact that the trace during those hours exhibited well defined minima at the operating frequency.

Conclusions

Considering that the ionospheric channel is a multipath time variant channel, the presented system is a very promising way to study its behavior.
 Moreover the use of a parametric algorithm to analyze the fading of the received power can give further capabilities to a basic vertical sounding system.

References

- Skolnik M.I., 1981. Introduction to radar systems. Mc GrawHill N.Y.
- Zuccheretti E., C. Bianchi, U. Sciacca, G. Tutone, B.J. Arokiasamy, 2003. The new AIS-INGV digital ionosonde. *Annals of Geophysics*, 46, n° 4, 647-659.
- Bianchi C., U. Sciacca, A. Zitzotti, E. Zuccheretti, B.J. Arokiasamy, 2003. Signal processing for phase-coded HF-VHF radars. *Annals of Geophysics*, 46, n° 4, 697-705.
- Goldsmith A. *Wireless communication*. Cambridge University Press, pp 644.
- Biglieri E., Proakis J., Sharma S. *Fading Channels: Information-Theoretic and Communications Aspects*. IEE Transactions on information theory, 44, n°6 1998.

Calibration

The ionosonde allows to appreciate power variation of ± 0.5 dB of the received echo. This resolution is obtained by a calibration of the system in a close loop configuration as in figure 13.

$$N = 10^{\frac{[E]}{20}} (cl + d)$$

Is the general form of the output of the system. Here:
 N is the value of the correlation peak.
 $[E]$ is the power at the receiver expressed in dBm.
 cl is the number of integration in the system.
 The calibration process aims to derive values for "c" and for "d".

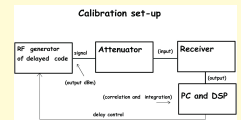


Figure 13. Close loop configuration

Varying the attenuation we generate different values for $[E]$ so to have different curves of N vs $[E]$ (as in fig 14.)

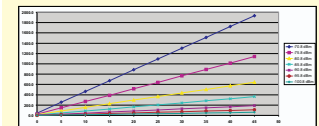


Figure 14

Dividing by the proper term containing power we should get a single line but, due to measurement errors, we have a distribution of lines from which we can derive "c" and "d" parameters with their own errors (fig. 15).

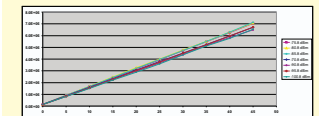


Figure 15

Particularly the best values for "c" and "d" are the expected values for the system.

$$[E] = 20 \cdot \log N - \log (cl + d)$$